

Regulation of ClC-K/barttin by endocytosis influences distal convoluted tubule hyperplasia

Clara Mayayo-Vallverdú¹ , Héctor Gaitán-Peñas^{2,3,4} , Mercedes Armand-Ugon^{2,3}, Ashraf Muhaisen^{2,3} , Esther Prat¹, Aida Castellanos^{2,3,4} , Xabier Elorza-Vidal^{2,3,4}, Miguel López de Heredia^{1,4} , Marta Alonso-Gardón^{2,3} , Carla Pérez-Rius^{2,3}, Marta Vecino-Pérez¹, Adrián Mallen⁵, Ekaitz Errasti-Murugarren¹, Miguel Hueso⁵ , Rafael Artuch^{4,6} , Virginia Nunes^{1,4,†} and Raúl Estévez^{2,3,4} 

¹Genes, Disease and Therapy Program, Molecular Genetics Laboratory-IDIBELL, Genetics Section, Department of Physiological Sciences, Faculty of Medicine and Health Sciences, University of Barcelona, Barcelona, Spain

²Physiology Unit, Department of Physiological Sciences, School of Medicine and Health Sciences, Institute of Neurosciences, University of Barcelona, L'Hospitalet de Llobregat, Spain

³Genes, Disease and Therapy Program, Physiology and pathology of the functional relationship between glia and neurons-IDIBELL, L'Hospitalet de Llobregat, Spain

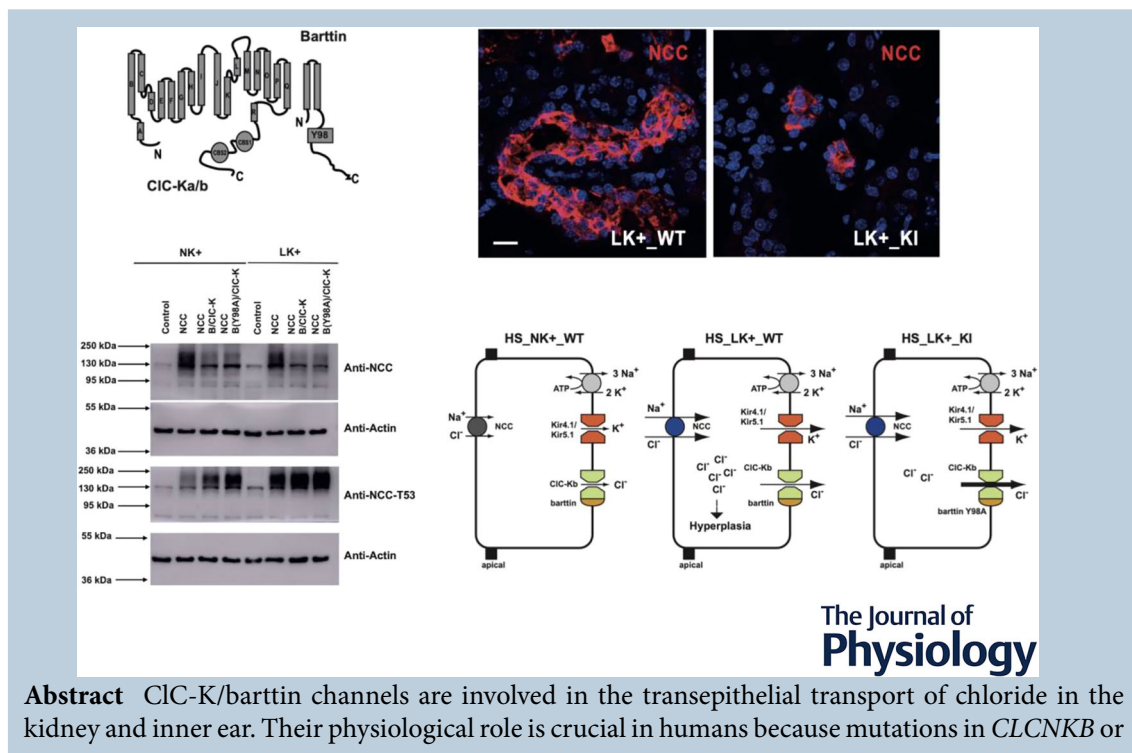
⁴Centro de Investigación en red de enfermedades raras (CIBERER), Instituto de Salud Carlos III, Madrid, Spain

⁵Department of Nephrology, Hospital Universitari Bellvitge and Institut d'Investigació Biomèdica de Bellvitge-IDIBELL, L'Hospitalet de Llobregat, Spain

⁶Institut de Recerca Sant Joan de Déu, Barcelona, Spain

Handling Editors: Peking Fong & Pawel Ferdek

The peer review history is available in the Supporting Information section of this article (<https://doi.org/10.1113/JP286729#support-information-section>).



C. Mayayo-Vallverdú and H. Gaitán-Peñas contributed equally to this work.

[†]Deceased.

BSND, encoding *ClC-Kb* and *barttin*, cause Bartter's syndrome types III and IV, respectively. *In vitro* experiments have shown that an amino acid change in a proline-tyrosine motif in the C-terminus of *barttin* stimulates *ClC-K* currents. The molecular mechanism of this enhancement and whether this potentiation has any *in vivo* relevance remains unknown. We performed electrophysiological and biochemical experiments in *Xenopus* oocytes and kidney cells co-expressing *ClC-K* and *barttin* constructs. We demonstrated that *barttin* possesses a YxxØ motif and, when mutated, increases *ClC-K* plasma membrane stability, resulting in larger currents. To address the impact of mutating this motif in kidney physiology, we generated a knock-in mouse. Comparing wild-type (WT) and knock-in mice under a standard diet, we could not observe any difference in *ClC-K* and *barttin* protein levels or localization, either in urinary or plasma parameters. However, under a high-sodium low-potassium diet, known to induce hyperplasia of distal convoluted tubules, knock-in mice exhibit reduced hyperplasia compared to WT mice. In summary, our *in vitro* and *in vivo* studies demonstrate that the previously identified PY motif is indeed an endocytic YxxØ motif in which mutations cause a gain of function of the channel.

(Received 11 April 2024; accepted after revision 11 July 2024; first published online 6 August 2024)

Corresponding author R. Estévez: Physiology Unit, Department of Physiological Sciences, School of Medicine and Health Sciences, Institute of Neurosciences, University of Barcelona-IDIBELL, C/Feixa Llarga s/n 08907 L'Hospitalet de Llobregat, Barcelona, Spain. Email: restevez@ub.edu

Abstract figure legend *ClC-K*/*barttin* channels mediate chloride transport in the kidney and inner ear. Mutating tyrosine 98 to alanine in *barttin* increases function by an unknown mechanism. In the present study, we performed experiments in oocytes and kidney cells, showing that tyrosine 98 is part of an endocytic motif. In addition, we show that mice containing this mutation showed a gain of function under specific conditions, resulting in lower proliferation of distal convoluted tubular cells. We suggest a mechanism that could explain this phenotype.

Key points

- It is revealed by mutagenesis and functional experiments that a previously identified proline-tyrosine motif regulating *ClC-K* plasma membrane levels is indeed an endocytic YxxØ motif.
- Biochemical characterization of mutants in the YxxØ motif in *Xenopus* oocytes and human embryonic kidney cells indicates that mutants showed increased plasma membrane levels as a result of an increased stability, resulting in higher function of *ClC-K* channels.
- Mutation of this motif does not affect *barttin* protein expression and subcellular localization *in vivo*.
- Knock-in mice with a mutation in this motif, under conditions of a high-sodium low-potassium diet, exhibit less hyperplasia in the distal convoluted tubule than wild-type animals, indicating a gain of function of the channel *in vivo*.

Clara Mayayo-Vallverdú graduated in Biology from the Pompeu Fabra University of Barcelona, Spain. She then obtained a Master's Degree in Genetics and Genomics from the University of Barcelona (UB) and subsequently joined the Human Molecular Genetic group at the Bellvitge Biomedical Research Institute. Her PhD was in the field of amino acid transporters in genetic diseases and mouse models. Since 2022, she has been a postdoctoral researcher and an associate professor at the UB. **Héctor Gaitán-Peñas** received his degree in Biology from the University of Alicante, Spain. He then obtained his Master's Degree in Integrative Physiology from the UB, Spain and subsequently joined the Physiology and Pathology of The Functional Relationship Between Glia and Neurons Group at UB. His PhD was in the field of chloride channels in genetic diseases and model organisms. Since 2020, he has been a postdoctoral researcher and holds an associate professor position at the UB.



Introduction

Human kidney chloride channels from the CLC family (CLC-Ka and CLC-Kb) are important for transcellular chloride transport in the nephron (Jentsch & Pusch, 2018). The CLC-Ka homolog (CLC-K1) is expressed in the thin ascending limb and medullary thick ascending limb (TAL) of the loop of Henle (Hennings et al., 2017; Uchida et al., 1995), whereas the CLC-Kb homolog (CLC-K2) is detected in the medullary and cortical portions of the TAL, the distal convoluted tubule (DCT), the intercalated cells of the connecting tubule and the collecting duct (Estévez et al., 2001; Hennings et al., 2017; Kobayashi et al., 2001). Their physiological function is revealed by the phenotype of knockout mouse models (Hennings et al., 2017; Matsumura et al., 1999) and by the presence of pathological mutations in *CLCNKB* in patients affected with Bartter's syndrome type III (Simon et al., 1997).

Both CLC-K channels are obligatorily associated with barttin (Estévez et al., 2001), a two-transmembrane protein encoded by the *BSND* gene (Birkenhäger et al., 2001), which increases their stability and plasma membrane (PM) levels (Hayama et al., 2003). Barttin knockout mice (Nomura et al., 2011; Rickheit et al., 2008) and Bartter's syndrome type IV patients, in which *BSND* is mutated (Birkenhäger et al., 2001), show reduced expression of both CLC-K channels, severe salt loss and deafness. Moreover, it has been shown in zebrafish that barttin localization also depends on CLC-K (Pérez-Rius et al., 2019). Importantly, several biochemical studies have identified which parts of the barttin protein and which residues are important for CLC-K channel exit from the endoplasmic reticulum and for modification of channel function (Scholl et al., 2006; Steinke et al., 2015a, 2015b; Stölting et al., 2015; Wojciechowski et al., 2015, 2018).

The regulation of CLC-K channels and its consequences are not yet fully elucidated. Several hormones such as insulin-like growth factor-1, angiotensin II or adenosine have been shown to influence CLC-K function (Stavniichuk et al., 2023). In addition, CLC-K channels are regulated by extracellular calcium and pH (Gradogna et al., 2010; Pinelli et al., 2016). It has been suggested that pH influence on CLC-Kb activity might be important in the regulation of salt reabsorption and HCO_3^- secretion by beta-intercalated cells (Pinelli et al., 2016).

Intracellular chloride levels in the DCT might indirectly affect salt reabsorption by modulating the activity of sodium/chloride cotransporters (NCC) (Castañeda-Bueno et al., 2022; Terker et al., 2015). One of the best described mechanisms involved in the regulation of NCC is the phosphorylation at key sites, which enhances transport activity, by inhibiting its ubiquitination and increasing PM levels (Meor Azlan et al., 2021). Phosphorylation of NCC is a result of the activity of Ste20-related proline-alanine-rich (i.e.

SPAK) and oxidative stress-responsive gene 1 (i.e. OSR1) kinases, which, in turn, are regulated by the with-no-lysine kinases (WNKs), mainly the isoform WNK4. It is known that WNKs possess a chloride binding motif, and a decrease in intracellular chloride concentration activates WNKs (Murillo-de-Ozores et al., 2022). As the main chloride channel in the basolateral side of the DCT is CLC-Kb/barttin, which is open at almost all voltages because of the lack of protopore gating, it has been proposed that intracellular chloride depends on the basolateral membrane potential, which depends on the potassium gradient (Su et al., 2020). Thus, a reduction in plasma potassium levels is sensed by Kir4.1/Kir5.1 channels (Terker et al., 2015). In this sense, mice with low expression levels of barttin showed impaired NCC phosphorylation when fed with a high-salt and low-potassium diet (Nomura et al., 2018).

Increased levels of salt in the diet affect blood pressure. In this regard, *CLC-K2* mRNA was moderately decreased in WT rats under a high-salt diet (Vitzthum et al., 2002). Furthermore, a polymorphism in *CLCNKB* (T481S) has been associated with high blood pressure in human populations, suggesting that it might be a gain of function mutation, although functional studies are not completely clear showing divergent results depending on the expression system (Sile et al., 2007, 2009).

Additionally, Estévez et al. (2001) reported that the cytoplasmic tail of barttin contains a proline-tyrosine motif (PQPPYVRL), the so-called PY motif, which is a binding site for ubiquitin ligases. Thus, when the tyrosine is mutated to alanine (Y98A), CLC-Ka/barttin and CLC-Kb/barttin currents increase (Estévez et al., 2001). It has been suggested that this mutation increased channel levels at the PM, possibly because the ubiquitin ligase Nedd4-2 could not bind to this motif (Embark et al., 2004).

In the present study, we first performed an *in vitro* biochemical characterization of the mechanism by which Y98A mutation increases channel surface expression, suggesting it is part of an endocytosis YxxØ motif rather than the previously considered PY motif. Then, we generated a knock-in (KI) mouse model of barttin containing this mutation and assayed its impact on renal function. Our results suggest that Y98A is a gain of function mutation in the CLC-K/barttin channel both *in vitro* and *in vivo*.

Methods

Molecular biology

Plasmids presented herein were constructed using standard molecular biology techniques employing recombinant PCR and the Multisite Gateway System (Invitrogen, Carlsbad, CA, USA). The integrity of all cloned constructs was confirmed by sequencing.

Generation of custom antibodies against ClC-Kb and barttin proteins

Immune sera against synthetic peptides from mouse ClC-Kb MEELVGLREGASKKPVPL(C), corresponding to amino acids 1–18 at the N-terminus, or (C)KKAISTLTNPPAPK, corresponding to the last amino acids at the C-terminus (coupling cysteine between parenthesis), and mouse barttin (C)PEQEEEDLYYGLPD and (C)PLPDKELGFEPDIQG, corresponding to amino acids 275–288 and 293–307 of the C-terminus, were raised in rabbits using the services provided by Eurogentec (Seraing, Belgium). After several boosts of immunization, the antibodies were affinity purified using the peptides covalently linked to Sulfolink (Thermo Fisher Scientific, Waltham, MA, USA). The polyclonal antibodies were tested by immunoblotting in human embryonic kidney (HEK) 293T cells expressing ClC-Kb and barttin.

Electrophysiology and luminescence-based surface assays in *Xenopus* oocytes

Oocytes were obtained by surgery from *Xenopus laevis* purchased from Xenopus Express (Vernassal, France). Oocytes were harvested from frogs that had been anaesthetized by tricaine (ethyl 3-aminobenzoate methanesulfonate salt; Sigma-Aldrich, Madrid, Spain) and the follicular layer was enzymatically removed by collagenase digestion during 3 h at 17°C. After surgery, frogs were allowed to recover from anaesthesia and suitable aftercare was given. Oocytes were maintained at 17°C in Barth's solution containing (in mM): 88 NaCl, 1 KCl, 0.82 MgSO₄, 0.41 CaCl₂, 0.33 Ca(NO₃)₂, 2.4 NaHCO₃ and 10 Hepes/Tris, pH 7.4, as well as 10 mg L⁻¹ of gentamycin. Each oocyte was injected with 10 ng of capped ClC-Ka or ClC-Kb complementary RNA and 5 ng of barttin. Measurements were carried out in ND96 medium (96 mM NaCl, 2 mM KCl, 1.8 mM CaCl₂, 1 mM MgCl₂ and 5 mM Hepes buffer at pH 7.4). Voltage was clamped between +80 and -100 mV for 0.8 s in 20 mV steps throughout. Currents were measured using a TEC-05X voltage amplifier and the CellWorks program (NPI Electronic, Tamm, Germany). Off-line analysis was performed using pCLAMP9 (Molecular Devices, Sunnyvale, CA, USA) and SigmaPlot (Systat Software Inc., San Jose CA, USA).

To measure the surface membrane expression of HA-tagged proteins, we used a chemiluminescence-based method. Oocytes were placed in ND96 medium containing 1% bovine serum albumin (BSA) for 30 min at 4°C, then incubated for 60 min at 4°C with 1 µg mL⁻¹ of rat monoclonal anti-HA antibody (3F10; Roche Diagnostics, Sant Cugat del Vallès, Barcelona) in 1% BSA-ND96, before being washed and incubated with horseradish peroxidase-conjugated secondary antibody

[donkey anti-rat IgG (H+L); Jackson ImmunoResearch, Newmarket, UK] in 1% BSA-ND96 for 30–60 min at 4°C. Oocytes were washed thoroughly (1% BSA at 4°C for 60 min) and transferred to ND96 without BSA. Individual oocytes were placed in 50 µL of Power Signal enzyme-linked immunosorbent assay (ELISA) solution (Thermo Fisher Scientific). Chemiluminescence was quantified in a Turner TD-20/20 luminometer (Turner Biosystems, Sunnyvale, CA, USA).

Cell culture, transfection and cell surface ELISA

HEK293T cells were grown in Duplecco's modified Eagle's medium containing (v/v) 10% fetal bovine serum (Sigma, St Louis, MO, USA) 1% glutamine and 1% penicillin/streptomycin at 37°C in a humidity-controlled incubator with 5% CO₂. Cells were transiently transfected with Transfectin Lipid Reagent (Bio-Rad, Madrid, Spain) in accordance with the manufacturer's instructions. Experiments were performed 48–72 h after cell transfection. Experiments with different media containing high or low potassium were performed as previously described (Terker et al., 2015). Cell surface ELISA was performed as previously described (Zerangue et al., 1999).

Functional expression in *Xenopus* oocytes and HEK293T cells

Capped complementary RNA of ClC channels (10 ng) and barttin (5 ng) were expressed in *Xenopus* oocytes as described. Mutations were introduced by recombinant PCR and sequenced. Measurements were carried out in ND96 medium for oocytes or in extracellular media containing (in mM): 140 NaCl, 2 MgSO₄, 3CaCl₂, 10 Hepes and 5 glucose, pH 7.3, as well as intracellular media containing (in mM): 130 NaCl, 2 MgSO₄, 2 EGTA and 10 Hepes, pH 7.3, for cells.

Animal procedures

The *Bsnc*^{Y95A/Y95A} KI mouse model was generated by editing the genome of C57BL/6J mice by a clustered regularly interspaced short palindromic repeats (CRISPR)/CRISPR-associated 9 (Cas9) system using the services of Taconic Biosciences (Germantown, NY, USA). Four nucleotides were changed from position c.282 to c.285 (CTAC to TGCA), resulting in a synonymous change p.Pro94Pro and the targeted missense change p.Tyr95Ala. Heterozygous *Bsnc*^{Y95A/+} mice were crossed to obtain WT and homozygous KI mice in the same background (C57BL/6J). Mice were maintained in a specific pathogen-free animal facility, in a temperature- and humidity-controlled room, under a 12:12 h light/dark photoperiod. Mice were housed by sex in groups of three to

five mice per cage with *ad libitum* access to drinking water and food (VRF1 P chow; Special Diets Services, UK, code: 801900). All experimental protocols were approved by the Animal Experimentation Ethics Committee of IDIBELL (AAALAC accredited facility, B9900010). On the last day, mice were anaesthetized with inhaled isoflurane (IsoFlo, 100% liquid). Once deep asleep, they were killed by intracardiac puncture with lithium heparin-coated syringes to obtain blood samples. Mice died by exsanguination and death was ensured by cervical dislocation. The abdominal cavity was then opened to remove the kidneys.

WT and KI mice weight was assessed weekly from weaning until 5 months of age to ensure that the introduced mutation did not affect mouse development ($N = 25$ per condition). Then, to monitor water intake, and urinary excretion levels and collect 24 h urine samples, mice were housed individually in metabolic cages for 4 days ($N = 6-7$ per condition). On the last day, mice were killed by intracardiac puncture using syringes coated with lithium heparin to obtain blood samples and remove kidneys. Blood samples were centrifuged for 10 min at 1500 g and 4°C to obtain plasma. One and a half kidneys were stored at -80°C for gene and protein expression analysis, and the other half was placed in 4% paraformaldehyde for overnight fixation for subsequent histological analysis.

To ensure increased urinary ions levels, high-sodium normal-potassium (HSNK+) or high-sodium low-potassium (HSLK+) diets were administered to *Bsnd*^{Y95A/Y95A} mice for 12 consecutive days ($N = 6-7$ per condition). Groups were randomized by separating litters and sexes equally. Diets were prepared by modifying the Ssniff diet (Soest, West Germany) to obtain a final concentration of 6% NaCl and 1% K+, for the HSNK+ diet, and 6% NaCl and 0.01% K+, for the HSLK+ diet. Mice had *ad libitum* access to drinking water and their corresponding diet. During the last 4 days of treatment, mice were placed in metabolic cages to monitor daily food and water intake, weight, and urinary excretion levels and collect individual urine samples. Then, mice were killed to obtain blood and kidney samples as described above.

Western blots and immunohistochemistry

Barttin and CIC-K antibodies were produced as described previously. NCC and phospho-NCC were from Abcam (Cambridge, UK) and Cayman Chemical (Ann Arbor, MI, USA), respectively. Actin and tubulin antibodies were from Millipore (Spain, Madrid). Western blots were performed as previously described using kidney membranes.

Anaesthetized adult animals were perfused through the left ventricle with phosphate-buffered saline followed by 4% paraformaldehyde in phosphate-buffered saline.

When comparing protein levels and localization, half kidneys were fixed by placing them in 4% paraformaldehyde for overnight fixation for subsequent histological analysis. Tissue samples were mounted in OCT compound (Tissue Tek; Sakura Finetek, Alphen aan den Rijn, The Netherlands) for cryosections and cut into 10 μm sections. Detection of proteins was performed as previously described (Estévez et al., 2001) and the analysis was performed by confocal microscopy (Zeiss, Oberkochen, Germany). Quantification was performed using ImageJ (NIH, Bethesda, MD, USA).

Gene expression analysis

Kidney RNA extraction and purification were performed using the Direct-zol RNA MiniPrep Plus kit (Zymo Research, Irvine, CA, USA). RNA was quantified with the Qubit RNA BR Assay Kit (Invitrogen) and 1 μg was retrotranscribed using the Transcriptor First Strand cDNA Synthesis Kit (Roche, Basel, Switzerland). A primer pair was designed for renin (5'-GGAGGAAGTGTTCTCTGTCTACTACA-3'; 5'-GCTACCTCCTAGCACACCCTC-3') and GADPH (5'-TGTCGGTCGTGGATCTGAC-3'; 5'-CCTGCTTCACCACCTTCTTG-3'). Gene expression was measured following the NZY Supreme qPCR Green Master Mix (NZYTech, Lisbon, Portugal) protocol and using the Light Cycler 480 Real-Time PCR System (Roche). Then, the relative quantification was determined using the Delta-Delta Ct ($2^{-\Delta\Delta\text{Ct}}$) method normalized by *Gapdh* expression (Livak & Schmittgen, 2001).

Determination of parameters in urine and blood

Plasma and urinary levels of chloride (Cl^-), sodium (Na^+), potassium (K^+), calcium (Ca^{2+}) and magnesium (Mg^{2+}) were detected by indirect potentiometry in an Allinity ci-series automated analyzer (Abbot, Abbott Park, IL, USA). Ion data were normalized per mmol of creatinine, determined using the Creatinine2 assay (049T9120). Urinary PGE₂ was measured using the PGE₂ ELISA Kit (Cayman Chemical) in accordance with the manufacturer's instructions, and urinary pH was determined using the 52 09 pH electrode for micro-samples (CRISON, Barcelona, Spain). Osmolarity was determined using a vapour-pressure osmometer (Model 3320 Osmometer; Tecil, Barcelona, Spain).

Statistical analysis

For each calculated value from different experiments, data indicate the mean \pm SD. Statistical analyses were performed using Prism (GraphPad Software Inc., San Diego, CA, USA). To estimate statistical

significance for experiments comparing two populations, we used a two-tailed unpaired Student's *t* test or a Wilcoxon–Mann–Whitney test. For experiments comparing three or more populations, we used one-way ANOVA with Bonferroni multiple comparison tests. The tests used and the respective *P* values are indicated where appropriate.

Results

A mutation in the Tyr 98 of barttin increases ClC-K plasma membrane levels

In *Xenopus* oocytes, when ClC-Ka was co-expressed with barttin containing a Y98A mutation in a putative PY motif at the proximal C terminus (Fig. 1A), higher current levels (about two-fold) were observed compared to ClC-Ka co-expressed with WT barttin (Fig. 1B). Previous reports have shown that in MDCK cells stably transfected with WT or Y98A barttin, higher PM levels were observed for barttin Y98A mutant (Hayama et al., 2003). To confirm these results in *Xenopus* oocytes, we measured the surface levels of ClC-K expressed alone or together with WT or Y98A barttin. Barttin co-expression enhanced the surface expression of ClC-Ka and this effect was strongly potentiated by the Y98A mutant (Fig. 1C). Previous studies have shown that barttin retained its stimulatory effect on ClC-K1 activity even after large C terminal truncations (Estévez et al., 2001). Thus, we analyzed whether the ClC-K1 channel function could also be further increased by the Y98A mutation in the context of the previously described barttin truncation in residue 115 (115X) (Estévez et al., 2001). Interestingly, the Y98A mutation dramatically increased ClC-K1 channel activity (more than 10 times) (Fig. 1D).

Moreover, we addressed whether this PY motif could be translated to a different protein (Fig. 1E). We fused the C-terminal residues 60 to 115 of barttin containing (or not) the Y98A mutation to the C-terminus of N-terminal HA-tagged β 2-adrenergic receptor (β 2-ADR) and assayed surface expression. As an internal control, we used the same receptor containing the C terminus of the Kir6.2 channel (Zerangue et al., 1999), which contains a WT endoplasmic reticulum (ER) retention signal (RKR) or the signal mutated to alanines (AAA, free from ER retention). Mutation Y98A in the fused β 2-ADR also increased surface expression of the barttin-fused receptor, indicating that the barttin putative PY motif regulates PM levels independently of the context.

Characterization of the proline-tyrosine motif in barttin

These functional effects of the barttin Y98A variant resemble that observed for the sodium channel ENaC

(Staub et al., 1997) or the chloride transporter ClC-5 (Schwake et al., 2001), where a PY motif involved in channel endocytosis was described (Fig. 2A). Thus, we decided to investigate this putative PY motif in more detail via mutagenesis studies. We performed a site-directed scanning mutagenesis approach on the barttin protein, mutating every single residue from proline 94 to leucine 101 to alanine, and co-expressed them with ClC-Ka (Fig. 2B). By contrast to that expected for a typical PY motif, individual mutations of prolines 94, 96 and 97 to alanine, or even the double mutant of prolines 96 and 97, did not potentiate ClC-Ka currents, as Y98A mutation did. Similarly, no activating effects were observed when mutating the other three residues (Q95, V99 and R100). However, an increase in ClC-Ka currents was observed when leucine 101 was mutated to alanine (Fig. 2B). Considering these mutagenesis studies, we conclude that the identified motif is not a PY motif but rather an endocytosis YxxØ motif. Interestingly, it has been found that Y98 residue can be phosphorylated (Paulo et al., 2015). Mimicking this phosphorylation by introducing a glutamate residue instead of the tyrosine (Y98E) resulted also in increased currents (Fig. 2B).

In agreement with its role as an endocytosis motif, incubation with brefeldin A (a known ER-Golgi protein trafficking inhibitor) indicated that Y98A barttin is more stable at the PM than WT barttin (Fig. 2C). Moreover, channel co-expression with dynamin dominant negative (known to limit the endocytosis process) (Fig. 2D) potentiated ClC-Ka/WT-barttin currents but not in ClC-Ka/Y98A-barttin. We conclude that ClC-K/barttin channels might cycle between the PM and intracellular vesicles through clathrin-mediated and dynamin-dependent endocytic pathways, as has been described for other renal channels such as AQP2 (Sun et al., 2002).

Analyzing the effect of mutating the YxxØ motif in mammalian cells

To confirm that the effects observed in *Xenopus* oocytes could also be extrapolated to kidney mammalian cells, we analyzed the PM expression of ClC-Kb co-expressed with WT or Y98A barttin in HEK293 cells. To ensure that all transfected cells equally expressed both proteins, we developed a construct where both cDNAs were fused through E2A sequences. Using a luminescence-based ELISA signal, we could show that ClC-Kb PM levels were higher when co-expressed with Y98A barttin (Fig. 3A).

To demonstrate that increased levels of the channel at the PM resulted in a gain of function causing reduced intracellular chloride levels, we used a previously described method (Terker et al., 2015). For that purpose, we expressed NCC alone or together with ClC-Kb/barttin

or ClC-Kb/Y98A-barttin in HEK cells. Then, cells were treated with normal-potassium (NK⁺) or low-potassium (LK⁺) medium and the ratio of NCC phosphorylated at position Thr 53/ total NCC was estimated by a western blot (Fig. 3B and C). As previously described (Terker et al., 2015), incubation with LK⁺ medium caused an increase in the phosphorylation of NCC, an increase that was

potentiated by the presence of ClC-Kb/barttin channels (Fig. 3B and C). Importantly, in cells incubated in NK⁺ medium, the expression of ClC-Kb/barttin increased the phosphorylation of NCC, an effect that was further potentiated by ClC-Kb/Y98A-barttin channels (Fig. 3B and C). This result again suggested the gain of function effect of Y98A-barttin in mammalian cells.

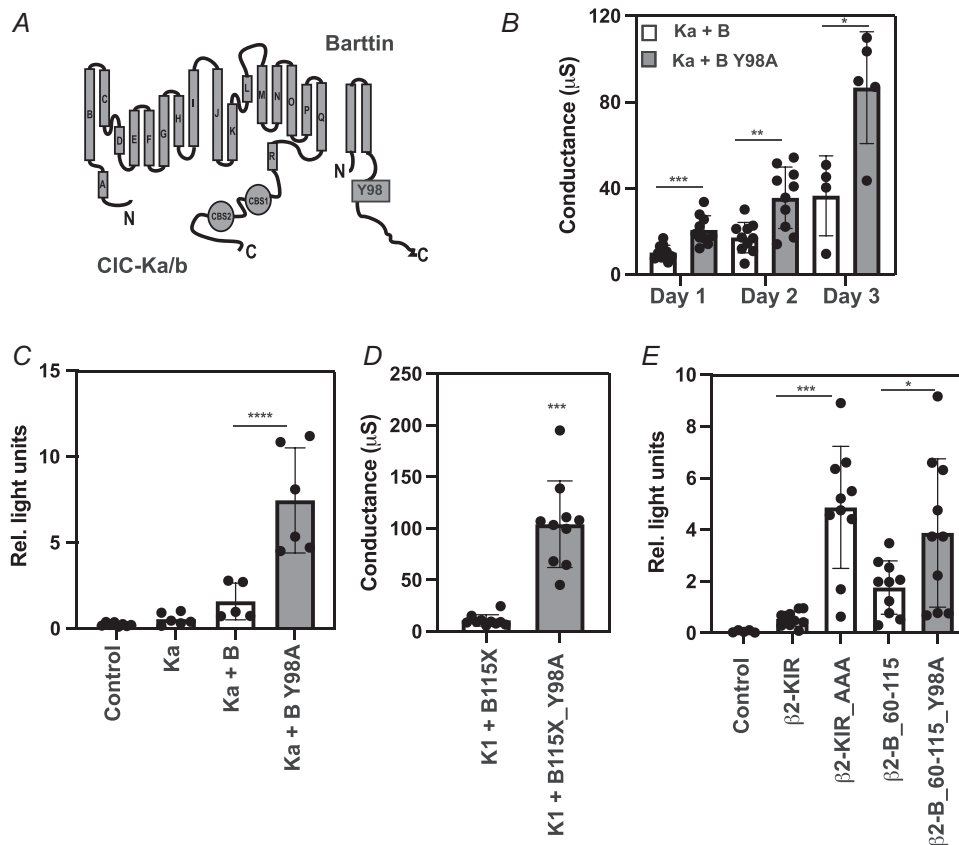


Figure 1. Functional characterization of a barttin Y98A mutant in *Xenopus oocytes*

A, schematic 2D models of the ClC-K chloride channel and barttin. The position of important structural features such as the helices and the cystathionine- β -synthase (CBS) domains are shown for the ClC-K protein. The localization of the N- and C-terminus is shown for both ClC-K and barttin proteins. The estimated position of the Y98 motif is highlighted in the barttin model. B, three-day time course of the conductance values mediated by ClC-Ka/barttin (Ka + B, white bars, $n = 9$ and $n = 4$, for days 1, 2 and 3, respectively) or ClC-Ka/barttin containing the Y98A mutation (Ka + B Y98A, black bars, $n = 9$, $n = 9$ and $n = 5$, for days 1, 2 and 3, respectively), after co-expression in *Xenopus oocytes*. An unpaired t test showed significant differences between Ka + B and Ka + B Y98A groups ($P < 0.0001$, $P = 0.00175$ and $P = 0.0141$, for days 1, 2 and 3, respectively). C, chemiluminescence assay for ClC-Ka plasma membrane levels estimation of Control ($n = 8$), ClC-Ka (Ka, $n = 6$), Ka + B ($n = 5$) and Ka + B Y98A ($n = 6$) groups. One-way ANOVA with Bonferroni multiple comparison tests was performed to compare the different groups. P values (vs. Ka group): control ($P > 0.999$), Ka + B ($P > 0.999$) and Ka + B Y98A ($P < 0.0001$). Importantly, significant differences were also found between Ka + B and Ka + B Y98A groups ($P < 0.0001$), indicating that ClC-Ka PM levels were further enhanced by Y98A barttin. D, conductance values mediated by ClC-K1 in co-expression with the truncated 115X version of barttin (K1 + B115X, $n = 10$) or barttin 115X additionally containing the Y98A mutation (K1 + B115X_Y98A, $n = 10$). An unpaired t test showed significant differences between K + B115X and K1 + B115X_Y98A ($P < 0.0001$). E, chemiluminescence assay monitoring N-terminal HA-tagged β 2-adrenergic receptor PM levels. Groups include control ($n = 5$) and C-terminal fusion of different residues, as follows: C-terminus of the WT Kir6.2 channel (β 2-KIR, $n = 10$) or Kir6.2 three-alanine mutation of retention signal (β 2-KIR_AAA, $n = 10$), and residues 60 to 115 of WT barttin (β 2-B_60-115, $n = 10$) or containing the Y98A mutation (β 2-B_60-115_Y98A, $n = 10$). Data represent the mean \pm SD. An unpaired t test showed significant differences between β 2-KIR and β 2-KIR_AAA ($P < 0.0001$) and between β 2-B_60-115 and β 2-B_60-115_Y98A ($P = 0.0422$). Significance: * $P \leq 0.05$, ** $P \leq 0.01$ and *** $P \leq 0.001$.

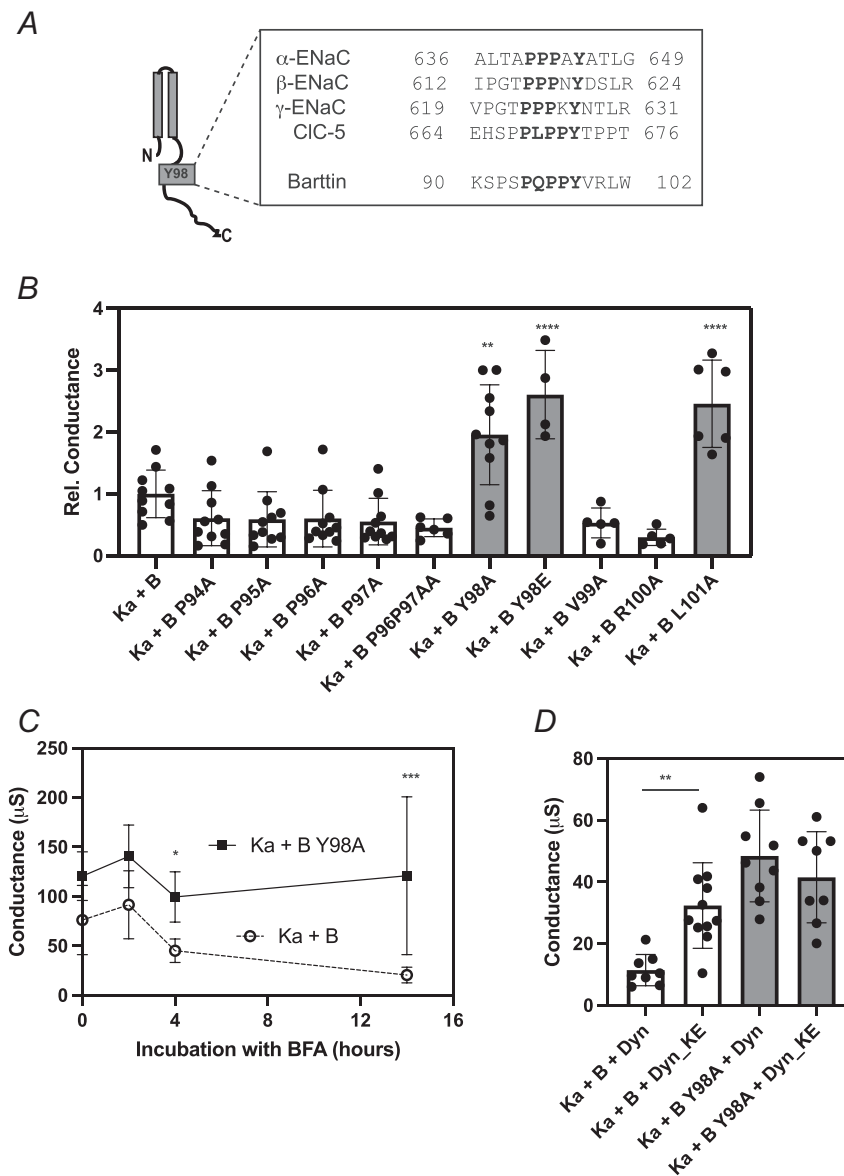


Figure 2. Determination of an endocytosis mutant in barttin

A, sequence magnification and alignment of the region surrounding and compressing the putative PY motif in barttin, CIC-5 and the ENaC channel. Motifs residues similarity is highlighted in bold letters. **B**, relative conductance values mediated by CIC-Ka in co-expression with WT barttin ($n = 10$) and different PY motif mutants. One-way ANOVA with Bonferroni multiple comparison tests was performed between the different groups. P values (vs. the Ka + B (WT) group): Ka + P94A ($n = 10$, $P > 0.999$), Ka + Q95A ($n = 10$, $P > 0.999$), Ka + P96A ($n = 10$, $P > 0.999$), Ka + P97A ($n = 10$, $P > 0.999$), Ka + P96P97AA ($n = 6$, $P > 0.999$), Ka + Y98A ($n = 10$, $P = 0.0258$), Ka + Y98E ($n = 4$, $P < 0.0001$), Ka + V99A ($n = 5$, $P > 0.999$), Ka + R100A ($n = 5$, $P = 0.637$) and Ka + L101A ($n = 6$, $P < 0.0001$). Groups showing enhanced conductance values are highlighted by black filled bars. In these groups, significance is indicated. **C**, time course of the conductance levels mediated by CIC-Ka/WT-barttin (Ka + B, $n = 7$, $n = 8$, $n = 8$ and $n = 7$, for incubation times of 0, 2, 4 and 14 h, respectively) and CIC-Ka/Y98A-barttin (Ka + B Y98A, $n = 6$, $n = 10$, $n = 10$ and $n = 6$, for incubation times of 0, 2, 4 and 14 h, respectively) in the presence of brefeldin A. One-way ANOVA with Bonferroni multiple comparison tests was performed to compare barttin WT vs. barttin Y98A effects at every brefeldin A incubation time. Significant differences were found after 4 h of incubation time: 0 h ($P = 0.618$), 2 h ($P = 0.0966$), 4 h ($P = 0.0371$) and 14 h ($P < 0.001$). **D**, conductance values mediated by CIC-Ka/WT-barttin (white bars) and CIC-Ka/Y98A-barttin (black filled bars) in co-expression with WT dynamin (Dyn) ($n = 8$ and $n = 9$, for WT and Y98A barttin variants, respectively) or dominant negative dynamin (Dyn_KE) ($n = 11$ and $n = 8$, for WT and Y98A barttin variants, respectively). One-way ANOVA with Bonferroni multiple comparison tests was performed comparing the dynamin variants effect. Significant differences were found for CIC-Ka/WT-barttin channels ($P = 0.00918$), whereas no significant differences were found for CIC-Ka/Y98A-barttin channels ($P > 0.999$). Data represent the mean \pm SD. Significance: * $P \leq 0.05$, ** $P \leq 0.01$ and *** $P \leq 0.001$.

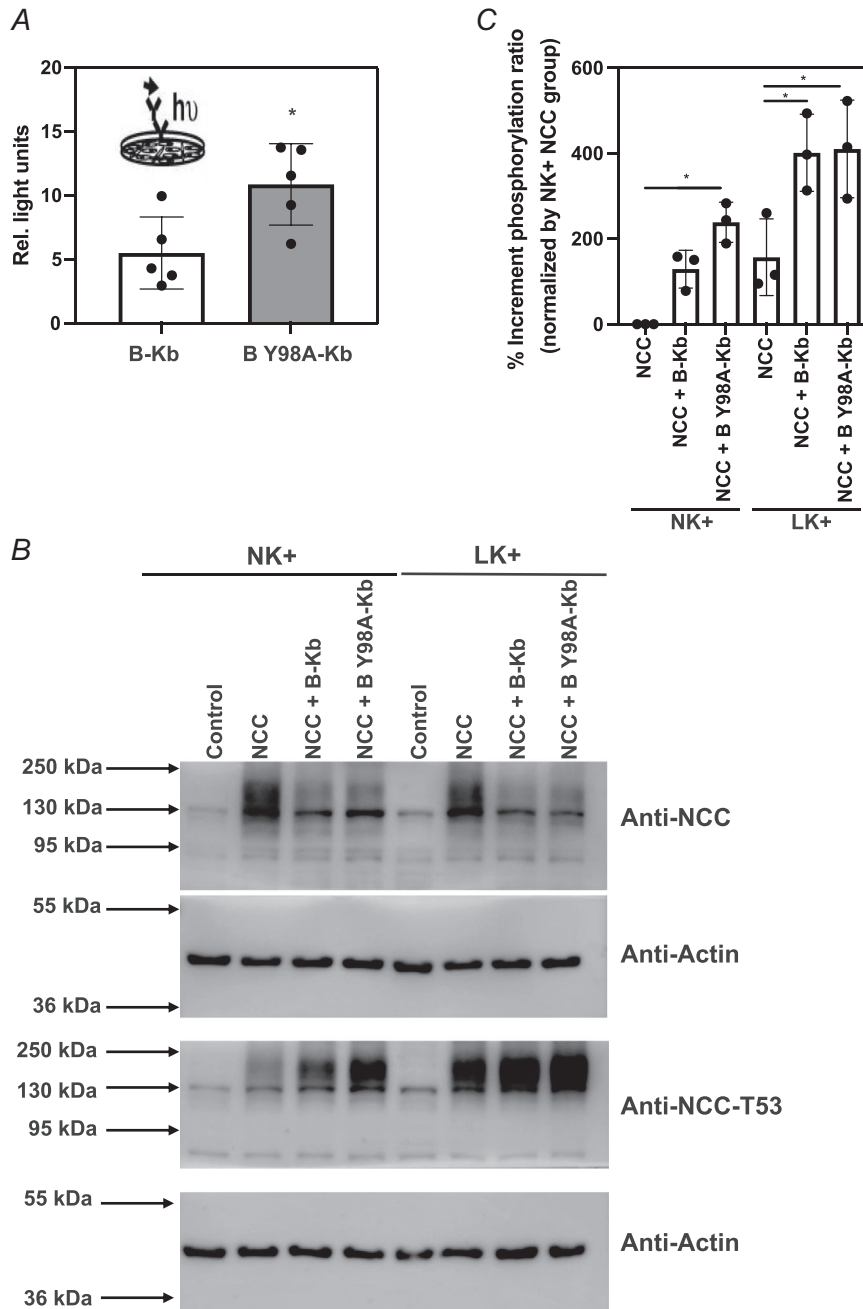


Figure 3. Characterization of barttin Y98A mutant in cells
 A, CIC-Kb relative PM levels estimation in both co-expression of WT-barttin (B-Kb, $n = 5$) or Y98A-barttin (B Y98A-Kb, $n = 5$). E2A fusion approach was applied to ensure the co-transfection of both barttin WT/Y98A and extracellular loop HA-tagged CIC-Kb channel proteins in all transfected cells. Data represent the mean \pm SD. An unpaired t test showed significant differences between both groups ($P < 0.0224$). Significance: * $P \leq 0.05$. Inset: illustration depicting the cell surface ELISA method selected to determine the relative PM levels of both groups (see methods). B, western blot detection of relative protein levels of NCC (Anti-NCC) and NCC phosphorylated at position Thr 53 (Anti-NCC-T53). Actin protein levels were detected as a loading control (Anti-Actin). Experiments were performed after expression of NCC alone or in co-expression with CIC-Kb/barttin (B-Kb) or CIC-Kb/Y98A-barttin (B Y98A-Kb) in HEK293T cells. Incubation conditions in normo-potassium (NK+) or low-potassium (LK+) medium are indicated at the top. C, western blot quantification of the increment (%) in the phosphorylation ratio of the NCC transporter (Th53/total NCC). Data of three independent experiments ($n = 3$) were normalized to the basal phosphorylation ratio exhibited by the NK+ NCC group. One-way ANOVA with Bonferroni multiple comparison tests was performed. P values of the

comparison of every group between NK+ and LK+ conditions, were: NCC ($P = 0.365$), NCC + B-CIC-Kb ($P = 0.0115$) and NCC + BY98A-Kb ($P = 0.234$). Under NK+ conditions, no significant differences in the phosphorylation ratio of NCC were found after B-Kb co-expression ($P = 0.839$). Conversely, B Y98A-Kb co-expression significantly increased the phosphorylation ratio of NCC ($P = 0.0307$), displaying no significant differences vs. the B-Kb co-expression group ($P > 0.999$). Under LK+ conditions, both B-CIC-Kb ($P = 0.0259$) and B Y98A-Kb ($P = 0.0199$) co-expression significantly increased the phosphorylation ratio of NCC, and no significant differences were found between B-Kb and B Y98A-Kb groups ($P > 0.999$).

Development of a *Bsnd* knock-in mouse with a mutation in the YxxØ motif

Once the role of the YxxØ motif as an internalization signal was described in two different cell systems, we aimed to assess the impact of this mutation *in vivo* by generating a *Bsnd*^{Y95A/Y95A} KI mouse (Fig. 4A). Homo-

zygous KI mice were born from heterozygous matings at Mendelian ratio, which were indistinguishable from their WT and heterozygous littermates, and their body weight evolution followed the same progression at different ages (Fig. 4B).

The expression and localization of CIC-K and barttin proteins were determined using Western blot and

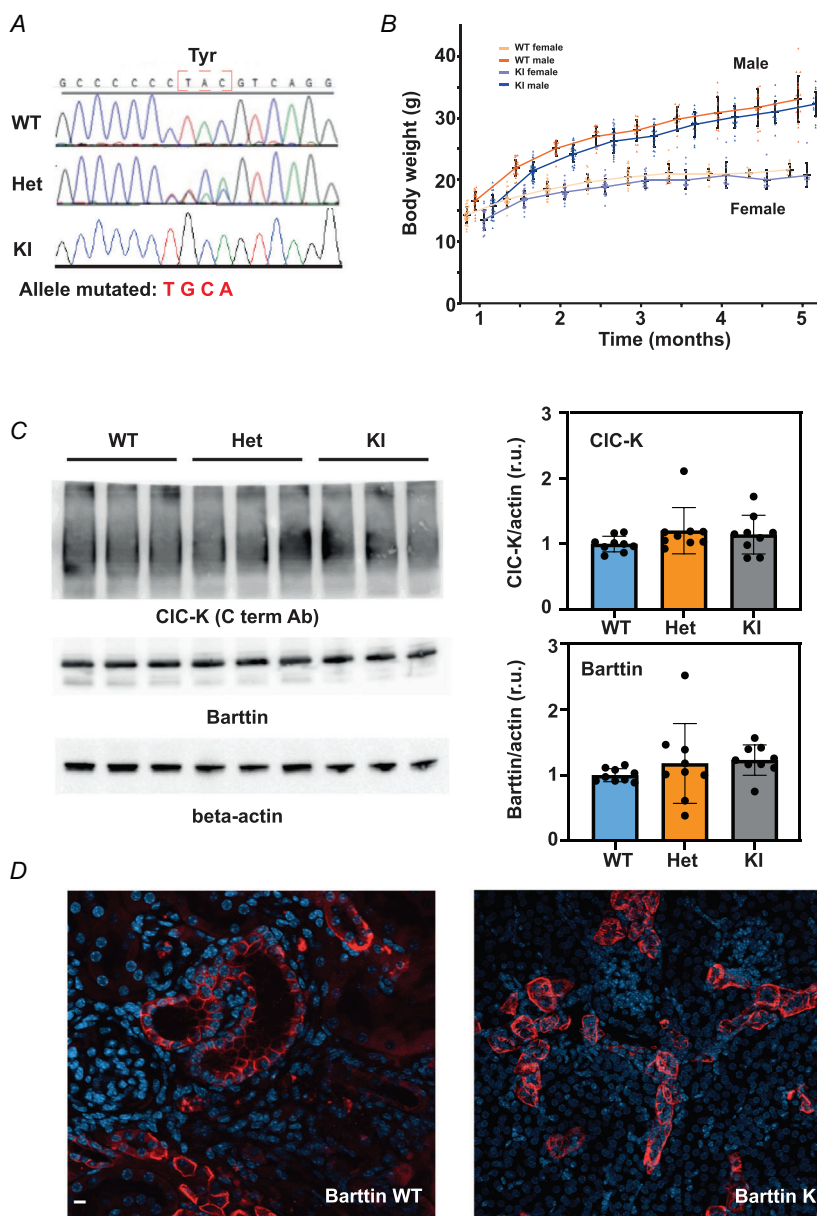


Figure 4. Generation and initial characterization of *Bsnd*^{Y95A/Y95A} KI mice

A, representative *Bsnd* sequences of wild-type (WT), heterozygous (Het) and knock-in (KI) mice. Changing the four nucleotides CTAC to TGCA by CRISPR-Cas9 results in the missense mutation p.Tyr95Ala. **B**, body weight evolution from the first to the fifth month of age, plotted by genotype and sex ($n = 25$). **C**, western blot detection (left) and quantification (right) of the relative protein levels of CIC-K2 and barttin proteins using our newly generated rabbit polyclonal antibodies. In the case of CIC-K2, the antibody against the synthetic C-terminal peptide was used (Rb#108). β -actin protein levels were detected as a loading control (beta-actin). A comparison of the renal tissue relative protein levels between WT, heterozygous (Het), and full knock-in mice (KI) is shown. Two bar diagrams show the normalized and β -actin corrected protein levels quantification of either the CIC-K2 channel and the barttin protein. Data represent the mean \pm SD ($n = 9$ in every group, three replicates out of three independent animals from each mice model). One-way ANOVA with Bonferroni multiple comparison tests showed no differences in the protein levels among: WT vs. Het ($P = 0.381$ and $P = 0.981$, for CIC-K2 and barttin, respectively), WT vs. KI ($P = 0.826$ and $P = 0.636$, for CIC-K2 and barttin, respectively) and Het vs. KI ($P > 0.999$ for both CIC-K2 and barttin). **D**, immunohistochemical staining of barttin in WT and KI mice renal tissue. Images show that barttin is in the basolateral side in WT and KI mice. Scale bar = 20 μ m. 4',6-Diamidino-2-phenylindole (i.e. DAPI) nuclei staining (blue) is also shown to help identify individual cells. [Colour figure can be viewed at wileyonlinelibrary.com]

immunofluorescence studies. Western blot analysis revealed no significant differences in protein expression between WT and KI mice (Fig. 4C). As previously shown, localization of both proteins in the KI mice was detected in the renal cortex and medulla in many segments such as the TAL or the cortical collecting duct (Fig. 4D). Staining of barttin in KI mice also showed basolateral expression in collecting duct cells resembling intercalated cells (Fig. 4D). Thus, we concluded that the mutation of the critical tyrosine does not affect either CIC-K/barttin expression or its subcellular localization *in vivo*.

We then addressed the functional consequences of the tyrosine mutation *in vivo* assessing different physiological parameters (Fig. 5). Measurements of urine volume, pH and osmolarity showed no differences between KI and WT mice (Fig. 5A). Water intake was also similar between both groups (Fig. 5A). Moreover, because the transcellular movement of chloride affects the movement of other ions such as sodium, potassium, magnesium and calcium, we assessed its concentration in urine and plasma (Table 1). No significant differences were observed in any ion comparison or blood urea nitrogen (Table 1).

Furthermore, in agreement with similar renin expression levels between the two genotypes, levels of PGE₂ were not significantly different (Fig. 5B).

Increasing salt delivery to the distal convoluted tubules in WT and KI mice

The above results showed no obvious differences in kidney functioning in *Bsnd*^{Y95A/Y95A} mice, although *in vitro* results have shown that this mutation increases CIC-K function. Considering the role of barttin in NCC phosphorylation on the DCT under a high-salt and low-potassium diet (HSLK+) (Nomura et al., 2018), we reasoned that differences might be observed under these conditions. Then, we fed WT and KI mice with a HSLK+ diet, and we used it as a control high-salt and normal potassium diet (HSNK+). We found that CIC-K levels slightly decreased in KI mice after the HSLK+ diet, whereas barttin remained unchanged. As expected for this HSLK+ treatment (Nomura et al., 2018), NCC phosphorylated levels were increased in both WT and KI. NCC levels were only slightly increased in KI

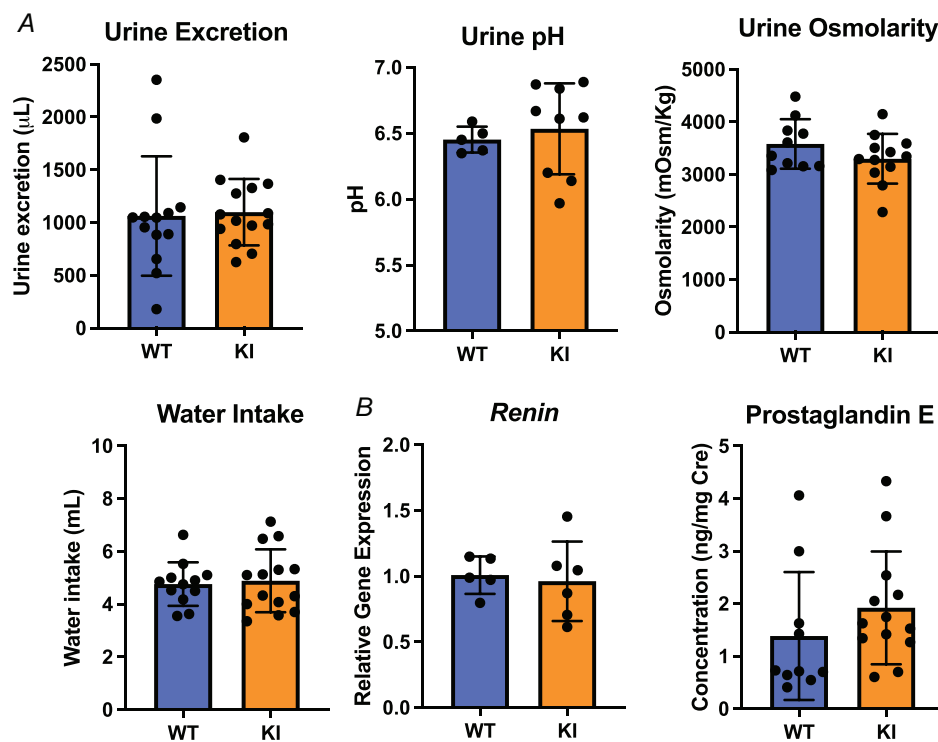


Figure 5. Characterization of urinary and salt-related parameters in *Bsnd*^{Y95A/Y95A} mice

A, comparison of urine excretion, pH, osmolarity (Osm) and water intake between wild-type (WT) and knock-in (KI) mice was assessed during the days housed individually in metabolic cages ($n = 11-14$). Osmolarity levels were normalized by body weight (kg). Water intake was measured in mL. B, *renin* gene expression ($n = 6-7$) and PGE₂ urinary normalized by mg of creatinine levels ($n = 10-12$). Data are expressed as the mean \pm SD and each dot represents a different mouse. No statistical differences were found between WT and KI after a Mann-Whitney-Wilcoxon test: urine excretion ($P = 0.550$), pH ($P = 0.364$), osmolarity ($P = 0.426$), water intake ($P = 0.910$), *renin* gene expression ($P = 0.166$) and PGE₂ ($P = 0.604$). [Colour figure can be viewed at www.oxfordjournals.org/doi/full/10.1093/ajph/134.10.1797]

Table 1. Ion levels in plasma and urine of WT and KI mice

	Plasma (mM)			Urine (mmol/mmolCre)		
	WT	KI	P-value	WT	KI	P value
Cl	112.00 ± 4.00	111.57 ± 2.93	0.617	83.62 ± 15.47	72.77 ± 12.45	0.610
Na	143.35 ± 4.89	145.61 ± 3.44	0.999	41.70 ± 5.39	36.21 ± 4.07	0.395
K	4.91 ± 0.67	4.98 ± 0.68	0.395	121.00 ± 25.80	106.33 ± 19.75	0.779
Ca	2.31 ± 0.09	2.33 ± 0.09	0.999	0.36 ± 0.08	0.41 ± 0.12	0.741
Mg	0.75 ± 0.07	0.84 ± 0.11	0.589	6.96 ± 2.12	7.71 ± 2.32	0.897
BUN (mg dL ⁻¹)	15.50 ± 2.05	17.92 ± 2.40	0.490			

Note: Values represent the mean ± SD, $n = 6-7$ mice per group. No statistical differences were found between WT and KI after a Mann–Whitney–Wilcoxon test. Plasma: Cl ($P = 0.617$), Na ($P = 0.999$), K ($P = 0.395$), Ca ($P = 0.999$), Mg ($P = 0.589$) and BUN ($P = 0.490$). Urine: Cl ($P = 0.610$), Na ($P = 0.395$), K ($P = 0.779$), Ca ($P = 0.741$) and Mg ($P = 0.897$). BUN = blood urea nitrogen (mg dL⁻¹).

mice (Fig. 6A). We observed only a tiny increase in the ratio between phosphorylated NCC and NCC for WT mice after a HSLK+ treatment. However, no significant differences were observed between WT and KI mice for barttin, ClC-K, total NCC and phosphorylated NCC levels (Fig. 6A).

In addition, it has been reported that an increase in the salt delivery to the DCT, especially under conditions of high salt and low potassium diet such as those used here, induces hyperplasia of the epithelial cells, manifested by increased numbers of cells in the tubules (de Bruyne, 2003; Kaissling & Stanton, 1988; Kaissling et al., 1985; Liang & Shimosawa, 2022; Saritas et al., 2018). In agreement with these findings, we observed a dramatic increase in the DCT area in WT and KI mice after HSLK+ vs. HSNK+ diet (Fig. 6B and C). Although KI mice also showed an increase in the DCT area, it was at a lower degree compared to WT animals in HSNK+ (Fig. 6B and C). Furthermore, quantification of the number of nuclei found on every individual DCT tubule, as revealed by 4',6-Diamidino-2-phenylindole (i.e. DAPI) staining, also showed much greater values in WT animals compared to KI animals in HSLK+ (Fig. 6D), whereas no differences were observed in HSNK+ or in KI animals when comparing HSLK+ vs. HSNK+. Quantification of the area/number of nuclei quotient showed an increased value for WT and KI animals in HSLK+ (Fig. 6E). Thus, both WT and KI DCT cells show an increased volume because of HSLK+. Accordingly, all of these results suggest that the increased DCT area in WT vs. KI animals could be attributed mainly to a major degree of hyperplasia.

Discussion

In the present study, we report the *in vitro* and *in vivo* effect of a motif in the C-terminus of barttin, which regulates the levels of ClC-K/barttin channels at the PM. Barttin C-terminus is poorly conserved between species and, even in zebrafish, the C-terminus is very

short and does not contain the motif investigated in the present study (Pérez-Rius et al., 2019). In mammals, in agreement with not having a functional role, large deletions of the C-terminus can be performed without abolishing the barttin function (Estévez et al., 2001). Nevertheless, truncating the human protein before residue 115 (115X) dramatically reduced its function (Estévez et al., 2001). In the context of the truncation 115X, we show here that adding the Y98A mutation also significantly increases ClC-K activity, suggesting that the distal C-terminus region may regulate the accessibility to the internalization motif; for example, by steric hindrance. Interestingly, many phospho-sites have been found in the C-terminus of barttin in different conditions, including residues in the motif described (Y98) or close to it (serine 107) (Paulo et al., 2015). We show here that mimicking the phosphorylation of this tyrosine, by mutating it to glutamate, increases macroscopic currents possibly by increasing PM channel levels. Thus, we suggest that it is possible that signalling cascades regulating the phosphorylation of barttin may influence PM levels of the complex.

In the case of the PY motif of ENaC and ClC-5 proteins, the increase in currents depended on reduced interactions with WW domains of ubiquitin protein ligases (Schwake et al., 2001; Staub et al., 1997). It has been shown in co-expression experiments that the ubiquitin ligase Nedd4-2 and the kinases SGK1 and 3 regulate ClC-K/barttin (Embark et al., 2004). However, recent studies with conditional knockout mice of Nedd4-2 indicated that barttin and ClC-K protein levels did not change (Nanami et al., 2018). Because we have shown that the internalization motif studied is a YxxØ motif instead of a PY motif, we conclude that the previously observed effects of Nedd4-2 on ClC-K currents might be through indirect mechanisms.

In vivo studies using the *Bsnd*^{Y95A/Y95A} mouse model showed no differences in ion levels or other physiological parameters under a normal diet between WT and KI mice.

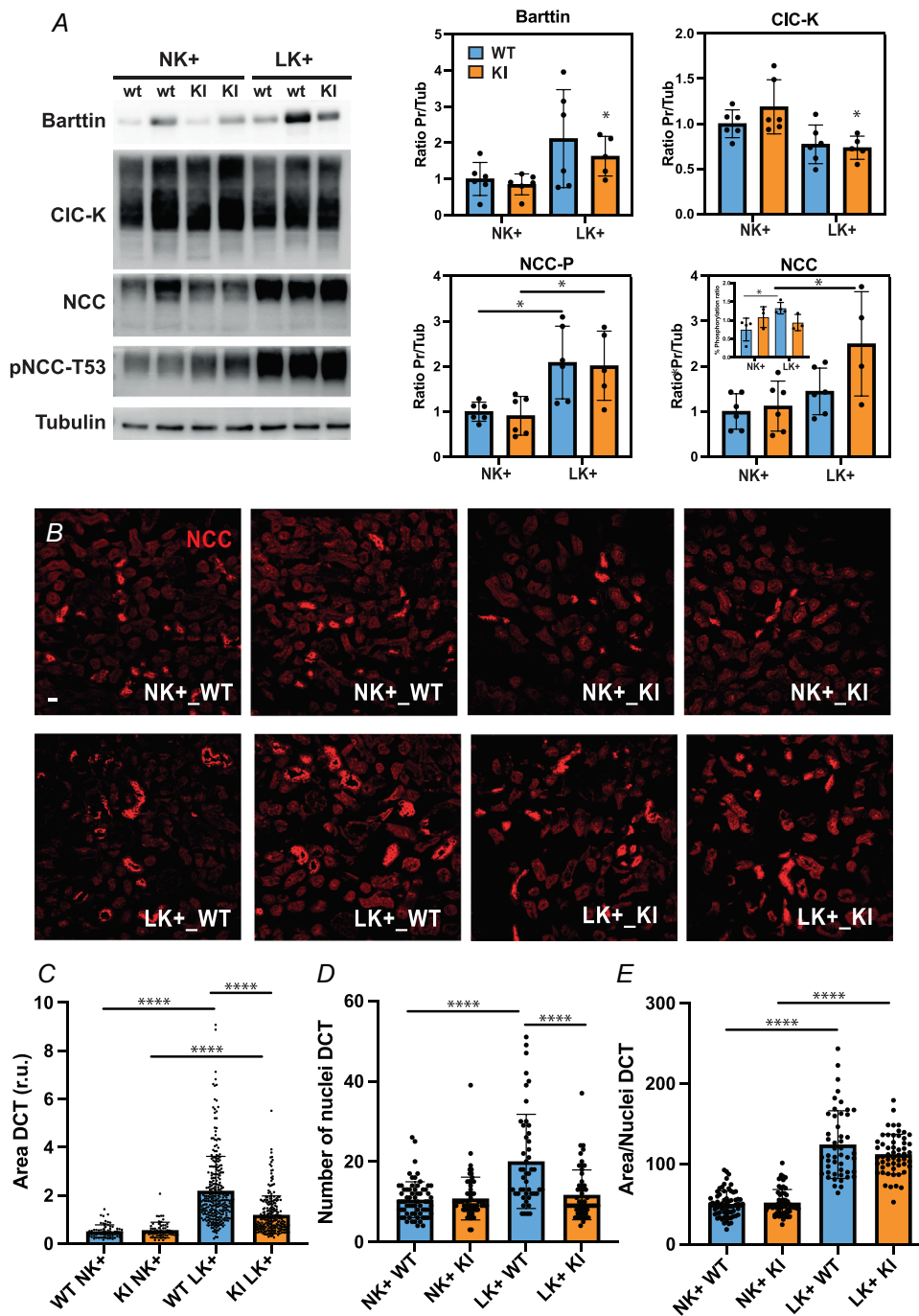


Figure 6. Effect of a high salt/low potassium diet in wild-type and *Bsn*^{ΔY95A/Y95A} mice
 A, western blot detection (left) and quantification (right) of the renal tissue relative protein levels of barttin, CIC-K2, NCC and phosphorylated NCC (pNCC-T53 or NCC-P). Tubulin protein levels were detected as a loading control. A comparison of the relative protein levels between WT and KI mice in both HSNK+ (NK+) and HSLK+ (LK+) diets is shown. Four bar diagrams show the normalized and tubulin corrected protein levels quantification of each of the proteins. An inset small diagram depicts the NCC-P/NCC ratio calculated for every group. One-way ANOVA with Bonferroni multiple comparison tests was performed. No significant differences were found in the protein levels between WT ($n = 6$ in all the groups) and KI mice ($n = 4$ in the NCC LK+ group, $n = 6$ in all the groups under NK+ diet and $n = 5$ in the rest of the groups under LK+ diet). P values (NK+ and LK+) as follows: Barttin ($P > 0.999$ and $P > 0.999$), CIC-K2 ($P = 0.868$ and $P > 0.999$), NCC-P ($P > 0.999$ and $P > 0.999$) and NCC ($P > 0.999$ and $P = 0.134$). Conversely, LK+ diet triggered significant alterations of protein levels in some groups. P values (WT and KI) as follows: Barttin ($P = 0.147$ and $P = 0.718$), CIC-K2 ($P = 0.479$ and $P = 0.0141$), NCC-P ($P = 0.0438$ and $P = 0.0515$) and NCC ($P > 0.999$ and $P = 0.0252$). Bar diagrams represent the mean \pm SD. Significance: * $P \leq 0.05$. B, immunohistochemical staining of the NCC cotransporter (red) allows to compare the distal convoluted

tubule areas between WT and full knock-in mice (KI) in both HSNK+ (NK+) and HSLK+ (LK+) diet conditions. Scale bar = 20 μm C–E, diagram graphs depicting the distal convoluted tubule area (C), number of nuclei quantifications (D) and area/nuclei quotient (E). One-way ANOVA with Bonferroni multiple comparison tests was performed. No significant differences were found in the distal convoluted tubule area between WT and KI mice fed with NK+ ($P > 0.999$, $n = 66$ and $n = 61$ for WT ($n = 3$ animals) and KI ($n = 4$ animals), respectively). Conversely, significant differences were found under LK+ diet ($P < 0.0001$, $n = 285$ and $n = 239$ for WT ($n = 6$ animals) and KI ($n = 5$ animals), respectively) diets. Furthermore, significant differences were found in the distal convoluted tubule area between NK+ and LK+ conditions, either in WT ($P < 0.0001$) and KI ($P < 0.001$) mice. Similarly, under NK+ diet, no significant differences were found in the quantified number of nuclei of distal convoluted tubules between WT ($n = 66$ ROIS, out of $n = 3$ animals) and KI mice ($n = 61$ ROIS, out of $n = 4$ animals) ($P > 0.999$); and, under LK+ diet, significant differences were found between WT ($n = 48$ ROIS, out of $n = 5$ animals) and KI mice ($n = 55$ ROIS, out of $n = 5$ animals) ($P < 0.0001$). Conversely, between NK+ and LK+ conditions, significant differences were found for the WT mice ($P < 0.0001$), whereas they were not significant for the KI ($P > 0.999$). In addition, no significant differences were found in the area/nuclei quotient between WT and KI mice fed with NK+ ($P > 0.999$, $n = 66$ and $n = 61$ for WT ($n = 3$ animals) and KI ($n = 4$ animals), respectively), or LK+ ($P > 0.121$, $n = 48$ and $n = 55$ for WT ($n = 5$ animals) and KI ($n = 5$ animals), respectively). Curiously, both WT and KI mice experienced a similar and significant increase in the area/nuclei quotient under LK+ diet ($P < 0.0001$ for both WT and KI). Significance: * $P \leq 0.05$, ** $P \leq 0.01$, *** $P \leq 0.001$ and **** $P \leq 0.0001$. [Colour figure can be viewed at wileyonlinelibrary.com]

In addition, we did not observe differences either in renin expression, PGE₂ or salt levels, suggesting that the blood pressure of KI mice should not be altered.

The regulation of NCC activity in the DCT is a key element for blood pressure and potassium homeostasis. The importance of this regulation can be clearly seen in genetic diseases (Castañeda-Bueno et al., 2022). Thus, overactivation of NCC in transgenic mouse models expressing WNK4 containing a Gordon syndrome mutation (Lalietti et al., 2006) led to increased blood pressure and blood potassium levels, and hyperplasia of the DCT. By contrast, the inactivation of NCC in

Gitelman's syndrome (Loffing et al., 2004) and Kir4.1 in EAST syndrome (Saritas et al., 2018), or thiazide treatment in rats (Loffing et al., 1995, 1996), which block NCC transporters, causes DCT atrophy. The mechanism of how levels of NCC transport activity are related to DCT remodelling is unknown. Under the HSLK+ diet, we identified reduced DCT hyperplasia levels in the KI mice vs. WT mice. Given that Y98A is a gain of function mutation in CIC-K/barttin channels, we hypothesize that intracellular chloride levels might affect tubule remodelling via yet-to-be-discovered mechanisms (Fig. 7). It could be that chloride accumulation affects

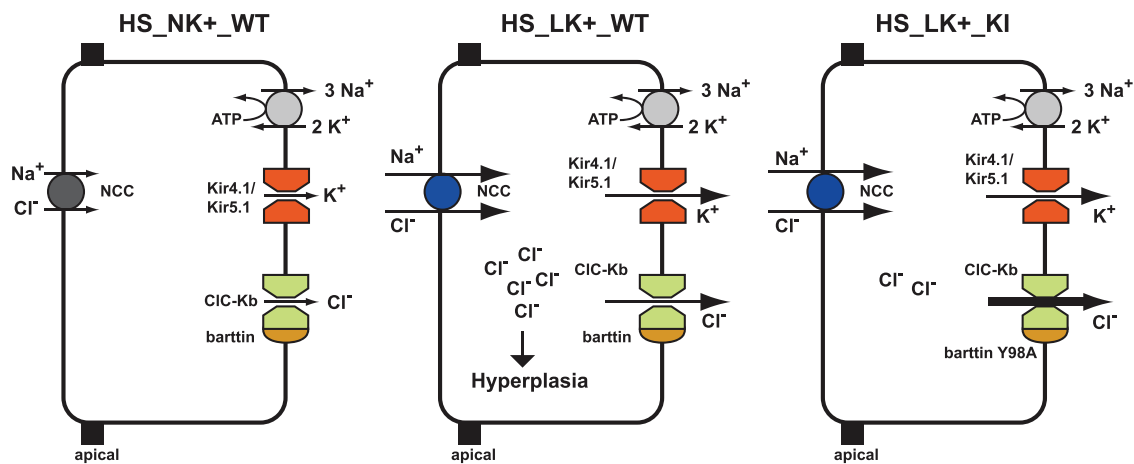


Figure 7. A model to explain the reduced DCT hyperplasia observed in *Bsnd*^{Y95A/Y95A} KI mice after a low potassium diet

Proposed model to explain the KI reduced DCT hyperplasia. In the left panel, the model illustrates the WT behaviour under HSNK+ conditions. Mid and right: WT and KI mice under HSLK+ treatment. HSLK+ stimulating conditions lead to an increased NCC activity (as a result of both an increased stability and phosphorylation state, depicted as a change in the transporter from black to blue colour), triggering a rise in the Cl⁻ and Na⁺ uptake. In the case of the WT mice (left), the activity of CIC-K/WT-barttin channels could be insufficient to mediate the needed Cl⁻ efflux into the bloodstream, thus leading to Cl⁻ accumulation in the cell cytoplasm. This could trigger a cell proliferation signal considered to be an alternative solution to overcome the Cl⁻ reabsorption needs by increasing the total number of distal convoluted tubular cells involved. Conversely (right), the gain-of-function exhibited by the CIC-K/Y98A-barttin channels might mediate higher Cl⁻ efflux, thus limiting its intracellular accumulation and the degree of cell proliferation triggered. [Colour figure can be viewed at wileyonlinelibrary.com]

intracellular sodium or simply NaCl reabsorption, which might influence cell volume. Changes in cell volume changes could affect renal volume-regulated anion channels influencing cell proliferation (Lopez-Cayuqueo et al., 2022). However, further studies should be performed to confirm these hypotheses.

In summary, considering both the *in vitro* results in oocytes and mammalian cells, as well as the *in vivo* effects identified in mice containing the Y98A variant, we suggest that mutations in the endocytic YxxØ motif of barttin lead to a gain of function of CLC-K/barttin channels. Thus, it could be possible that signalling cascades might regulate CLC-K/barttin channel function by directly or indirectly affecting its PM levels through the modulation of this motif. Further studies will explore this possibility and its biomedical implications.

References

- Birkenhäger, R., Otto, E., Schürmann, M. J., Vollmer, M., Ruf, E. M., Maier-Lutz, I., Beekmann, F., Fekete, A., Omran, H., Feldmann, D., Milford, D. V., Jeck, N., Konrad, M., Landau, D., Knoers, N., Antignac, C., Sudbrak, R., Kispert, A., & Hildebrandt, F. (2001). Mutation of BSND causes Bartter syndrome with sensorineural deafness and kidney failure. *Nature Genetics*, **29**(3), 310–314.
- Castañeda-Bueno, M., Ellison, D. H., & Gamba, G. (2022). Molecular mechanisms for the modulation of blood pressure and potassium homeostasis by the distal convoluted tubule. *European Molecular Biology Organization Molecular Medicine*, **14**(2), e14273.
- de Bruyne, L. K. M. (2003). Mechanisms and management of diuretic resistance in congestive heart failure. *Postgraduate Medical Journal*, **79**(931), 268–271.
- Embark, H. M., Böhmer, C., Palmada, M., Rajamanickam, J., Wyatt, A. W., Wallisch, S., Capasso, G., Waldegger, P., Seyberth, H. W., Waldegger, S., & Lang, F. (2004). Regulation of CLC-Ka/barttin by the ubiquitin ligase Nedd4-2 and the serum- and glucocorticoid-dependent kinases. *Kidney International*, **66**(5), 1918–1925.
- Estévez, R., Boettger, T., Stein, V., Birkenhäger, R., Otto, E., Hildebrandt, F., & Jentsch, T. J. (2001). Barttin is a Cl⁻ channel β -subunit crucial for renal Cl⁻ reabsorption and inner ear K⁺ secretion. *Nature*, **414**(6863), 558–561.
- Gradogna, A., Babini, E., Picollo, A., & Pusch, M. (2010). A regulatory calcium-binding site at the subunit interface of CLC-K kidney chloride channels. *Journal of General Physiology*, **136**(3), 311–323.
- Hayama, A., Rai, T., Sasaki, S., & Uchida, S. (2003). Molecular mechanisms of Bartter syndrome caused by mutations in the BSND gene. *Histochemistry and Cell Biology*, **119**(6), 485–493.
- Hennings, J. C., Andriani, O., Picard, N., Paulais, M., Huebner, A. K., Cayuqueo, I. K. L., Bignon, Y., Keck, M., Cornière, N., Böhm, D., Jentsch, T. J., Chambrey, R., Teulon, J., Hübner, C. A., & Eladari, D. (2017). The CLC-K2 chloride channel is critical for salt handling in the distal nephron. *Journal of the American Society of Nephrology*, **28**(1), 209–217.
- Jentsch, T. J., & Pusch, M. (2018). CLC chloride channels and transporters: Structure, function, physiology, and disease. *Physiological Reviews*, **98**(3), 1493–1590.
- Kaissling, B., Bachmann, S., & Kriz, W. (1985). Structural adaptation of the distal convoluted tubule to prolonged furosemide treatment. *American Journal of Physiology*, **248**(3 Pt 2), F374–F381.
- Kaissling, B., & Stanton, B. A. (1988). Adaptation of distal tubule and collecting duct to increased sodium delivery. *I Ultrastructure*, **255**(6 Pt 2), F1269–F1275.
- Kobayashi, K., Uchida, S., Mizutani, S., Sasaki, S., & Marumo, F. (2001). Intrarenal and cellular localization of CLC-K2 protein in the mouse kidney. *Journal of the American Society of Nephrology*, **12**(7), 1327–1334.
- Lalio, M. D., Zhang, J., Volkman, H. M., Kahle, K. T., Hoffmann, K. E., Toka, H. R., Nelson-Williams, C., Ellison, D. H., Flavell, R., Booth, C. J., Lu, Y., Geller, D. S., & Lifton, R. P. (2006). Wnk4 controls blood pressure and potassium homeostasis via regulation of mass and activity of the distal convoluted tubule. *Nature Genetics*, **38**(10), 1124–1132.
- Liang, L., & Shimosawa, T. (2022). Molecular mechanisms of Na-Cl cotransporter in relation to hypertension in chronic kidney disease. *International Journal of Molecular Sciences*, **24**(1), 286.
- Livak, K. J., & Schmittgen, T. D. (2001). Analysis of relative gene expression data using real-time quantitative PCR and the 2(-Delta Delta C(T)) method. *Methods (San Diego, California)*, **25**(4), 402–408.
- Loffing, J., Le Hir, M., & Kaissling, B. (1995). Modulation of salt transport rate affects DNA synthesis *in vivo* in rat renal tubules. *Kidney International*, **47**(6), 1615–1623.
- Loffing, J., Loffing-Cueni, D., Hegyi, I., Kaplan, M. R., Hebert, S. C., Le Hir, M., & Kaissling, B. (1996). Thiazide treatment of rats provokes apoptosis in distal tubule cells. *Kidney International*, **50**(4), 1180–1190.
- Loffing, J., Vallon, V., Loffing-Cueni, D., Aregger, F., Richter, K., Pietri, L., Bloch-Faure, M., Hoenderop, J. G. J., Shull, G. E., Meneton, P., & Kaissling, B. (2004). Altered renal distal tubule structure and renal Na(+) and Ca(2+) handling in a mouse model for Gitelman's syndrome. *Journal of the American Society of Nephrology*, **15**(9), 2276–2288.
- Lopez-Cayuqueo, K. I., Planells-Cases, R., Pietzke, M., Oliveras, A., Kempa, S., Bachmann, S., & Jentsch, T. J. (2022). Renal deletion of LRRC8/VRAC channels induces proximal tubulopathy. *Journal of the American Society of Nephrology*, **33**(8), 1528–1545.
- Matsumura, Y., Uchida, S., Kondo, Y., Miyazaki, H., Ko, S. B. H., Hayama, A., Morimoto, T., Liu, W., Arisawa, M., Sasaki, S., & Marumo, F. (1999). Overt nephrogenic diabetes insipidus in mice lacking the CLC-K1 chloride channel. *Nature Genetics*, **21**(1), 95–98.
- Meor Azlan, N. F., Koeners, M. P., & Zhang, J. (2021). Regulatory control of the Na-Cl co-transporter NCC and its therapeutic potential for hypertension. *Acta Pharmaceutica Sinica B*, **11**(5), 1117–1128.

- Murillo-de-Ozores, A. R., Carbajal-Contreras, H., Magaña-Ávila, G. R., Valdés, R., Grajeda-Medina, L. I., Vázquez, N., Zariñán, T., López-Saavedra, A., Sharma, A., Lin, D. H., Wang, W. H., Delpire, E., Ellison, D. H., Gamba, G., & Castañeda-Bueno, M. (2022). Multiple molecular mechanisms are involved in the activation of the kidney sodium-chloride cotransporter by hypokalemia. *Kidney International*, **102**(5), 1030–1041.
- Nanami, M., Pham, T. D., Kim, Y. H., Yang, B., Sutliff, R. L., Staub, O., Klein, J. D., Lopez-Cayuqueo, K. I., Chambrey, R., Park, A. Y., Wang, X., Pech, V., Verlander, J. W., & Wall, S. M. (2018). The role of intercalated cell Nedd4–2 in BP regulation, ion transport, and transporter expression. *Journal of the American Society of Nephrology*, **29**(6), 1706–1719.
- Nomura, N., Shoda, W., Wang, Y., Mandai, S., Furusho, T., Takahashi, D., Zeniya, M., Sohara, E., Rai, T., & Uchida, S. (2018). Role of ClC-K and barttin in low potassium-induced sodium chloride cotransporter activation and hypertension in mouse kidney. *Bioscience Reports*, **38**(1), BSR20171243.
- Nomura, N., Tajima, M., Sugawara, N., Morimoto, T., Kondo, Y., Ohno, M., Uchida, K., Mutig, K., Bachmann, S., Soleimani, M., Ohta, E., Ohta, A., Sohara, E., Okado, T., Rai, T., Jentsch, T. J., Sasaki, S., & Uchida, S. (2011). Generation and analyses of R8L barttin knockin mouse. *American Journal of Physiology-Renal Physiology*, **301**(2), F297–307.
- Paulo, J. A., Mcallister, F. E., Everley, R. A., Beausoleil, S. A., Banks, A. S., & Gygi, S. P. (2015). Effects of MEK inhibitors GSK1120212 and PD0325901 in vivo using 10-plex quantitative proteomics and phosphoproteomics. *Proteomics*, **15**(2–3), 462–473.
- Pérez-Rius, C., Castellanos, A., Gaitán-Peñas, H., Navarro, A., Artuch, R., Barrallo-Gimeno, A., & Estévez, R. (2019). Role of zebrafish ClC-K/barttin channels in apical kidney chloride reabsorption. *Journal of Physiology*, **597**(15), 3969–3983.
- Pinelli, L., Nissant, A., Edwards, A., Lourdel, S., Teulon, J., & Paulais, M. (2016). Dual regulation of the native ClC-K2 chloride channel in the distal nephron by voltage and pH. *Journal of General Physiology*, **148**(3), 213–226.
- Rickheit, G., Maier, H., Strenzke, N., Andreescu, C. E., De Zeeuw, C. I., Muenscher, A., Zdebik, A. A., & Jentsch, T. J. (2008). Endocochlear potential depends on Cl⁻ channels: Mechanism underlying deafness in Bartter syndrome IV. *European Molecular Biology Organization Journal*, **27**(21), 2907–2917.
- Saritas, T., Puelles, V. G., Su, X. T., McCormick, J. A., Welling, P. A., & Ellison, D. H. (2018). Optical clearing in the kidney reveals potassium-mediated tubule remodeling. *Cell Reports*, **25**(10), 2668–2675.e3.
- Scholl, U., Hebeisen, S., Janssen, A. G. H., Müller-Newen, G., Alekov, A., & Fahlke, C. (2006). Barttin modulates trafficking and function of ClC-K channels. *The Proceedings of the National Academy of Sciences*, **103**(30), 11411–11416.
- Schwake, M., Friedrich, T., & Jentsch, T. J. (2001). An internalization signal in ClC-5, an endosomal Cl⁻ channel mutated in dent's disease. *Journal of Biological Chemistry*, **276**(15), 12049–12054.
- Sile, S., Gillani, N. B., Velez, D. R., Vanoye, C. G., Yu, C., Byrne, L. M., Gainer, J. V., Brown, N. J., Williams, S. M., & George, A. L. (2007). Functional BSND variants in essential hypertension. *American Journal of Hypertension*, **20**(11), 1176–1182.
- Sile, S., Velez, D. R., Gillani, N. B., Narsia, T., Moore, J. H., George, A. L., Vanoye, C. G., & Williams, S. M. (2009). CLCNKB-T481S and essential hypertension in a Ghanaian population. *Journal of Hypertension*, **27**(2), 298–304.
- Simon, D. B., Bindra, R. S., Mansfield, T. A., Nelson-Williams, C., Mendonca, E., Stone, R., Schurman, S., Nayir, A., Alpay, H., Bakkaloglu, A., Rodriguez-Soriano, J., Morales, J. M., Sanjad, S. A., Taylor, C. M., Pilz, D., Brem, A., Trachtman, H., Griswold, W., Richard, G. A., ... Lifton, R. P. (1997). Mutations in the chloride channel gene, CLCNKB, cause Bartter's syndrome type III. *Nature Genetics*, **17**(2), 171–178.
- Staub, O., Gautschi, I., Ishikawa, T., Breitschopf, K., Ciechanover, A., Schild, L., & Rotin, D. (1997). Regulation of stability and function of the epithelial Na⁺ channel (ENaC) by ubiquitination. *European Molecular Biology Organization Journal*, **16**(21), 6325–6336.
- Stavniichuk, A., Pyrshev, K., Tomilin, V. N., Kordysh, M., Zaika, O., & Pochynyuk, O. (2023). Modus operandi of ClC-K2 Cl⁻ channel in the collecting duct intercalated cells. *Biomolecules*, **13**(1), 177.
- Steinke, K. V., Gorinski, N., Wojciechowski, D., Todorov, V., Guseva, D., Ponimaskin, E., Fahlke, C., & Fischer, M. (2015a). Human ClC-K channels require palmitoylation of their accessory subunit barttin to be functional. *Journal of Biological Chemistry*, **290**, 17390–17400.
- Steinke, K. V., Gorinski, N., Wojciechowski, D., Todorov, V., Guseva, D., Ponimaskin, E., Fahlke, C., & Fischer, M. (2015b). Human ClC-K channels require palmitoylation of their accessory subunit barttin to be functional. *Journal of Biological Chemistry*, **290**, 17390–17400.
- Stöltzing, G., Bungert-Plümke, S., Franzen, A., & Fahlke, C. (2015). Carboxyl-terminal truncations of ClC-Kb abolish channel activation by barttin via modified common gating and trafficking. *Journal of Biological Chemistry*, **290**, 30406–30416.
- Su, X. T., Klett, N. J., Sharma, A., Allen, C. N., Wang, W. H., Yang, C. L., & Ellison, D. H. (2020). Distal convoluted tubule Cl⁻ concentration is modulated via K⁺ channels and transporters. *American Journal of Physiology-Renal Physiology*, **319**, F534–F540.
- Sun, T. X., Van Hoek, A., Huang, Y., Bouley, R., McLaughlin, M., & Brown, D. (2002). Aquaporin-2 localization in clathrin-coated pits: Inhibition of endocytosis by dominant-negative dynamin. *American Journal of Physiology-Renal Physiology*, **282**(6), F998–1011.
- Terker, A. S., Zhang, C., McCormick, J. A., Lazelle, R. A., Zhang, C., Meermeier, N. P., Siler, D. A., Park, H. J., Fu, Y., Cohen, D. M., Weinstein, A. M., Wang, W. H., Yang, C. L., & Ellison, D. H. (2015). Potassium modulates electrolyte balance and blood pressure through effects on distal cell voltage and chloride. *Cell Metabolism*, **21**(1), 39–50.

- Uchida, S., Sasaki, S., Nitta, K., Uchida, K., Horita, S., Nihei, H., & Marumo, F. (1995). Localization and functional characterization of rat kidney-specific chloride channel, ClC-K1. *Journal of Clinical Investigation*, **95**(1), 104–113.
- Vitzthum, H., Castrop, H., Meier-Meitingner, M., Riegger, G. A. J., Kurtz, A., Krämer, B. K., & Wolf, K. (2002). Nephron specific regulation of chloride channel ClC-K2 mRNA in the rat. *Kidney International*, **61**(2), 547–554.
- Wojciechowski, D., Fischer, M., & Fahlke, C. (2015). Tryptophan scanning mutagenesis identifies the molecular determinants of distinct barttin functions. *Journal of Biological Chemistry*, **290**(30), 18732–18743.
- Wojciechowski, D., Thiemann, S., Schaal, C., Rahtz, A., de la Roche, J., Begemann, B., Becher, T., & Fischer, M. (2018). Activation of renal ClC-K chloride channels depends on an intact N terminus of their accessory subunit barttin. *Journal of Biological Chemistry*, **293**(22), 8626–8637.
- Zerangue, N., Schwappach, B., Yuh, N. J., & Lily, Y. J. (1999). A new ER trafficking signal regulates the subunit stoichiometry of plasma membrane K(ATP) channels. *Neuron*, **22**(3), 537–548.

Additional information

Data availability statement

All of the data are accessible in an Excel file provided in the Supplementary information.

Competing interests

The authors declare that they have no competing interests.

Author contributions

R.E. designed the study and wrote the manuscript. All authors have approved the final version of the manuscript submitted for

publication and agree to be accountable for all aspects of the work. All persons designated as authors qualify for authorship, and all those who qualify for authorship are listed.

Funding

None.

Acknowledgements

This work was supported in part by: MICINN projects RTI2018-093493-B-I00 and PID2021-126246NB-I00 to RE and two CIBERER intramural projects to RE, VN and RA. RA was supported by Carmen de Torres Grants-IRSJD. We thank Dr Thomas Jentsch for support in the initial stages of this project in Hamburg at the ZMNH. We thank Dr Blanche Schwappach for the plasmids of β 2ADR receptor.

Keywords

barttin, chloride channels, ClC-K, distal convoluted tubule, endocytosis, gain of function mutation, knock-in mouse

Supporting information

Additional supporting information can be found online in the Supporting Information section at the end of the HTML view of the article. Supporting information files available:

Peer Review History

Supplementary information